

# Quantitative limitation of active site and characteristics of chemical oxidized well-aligned carbon nanotubes

Tsung-Chi Hung<sup>a,\*</sup>, Chia-Fu Chen<sup>a,d</sup>, Mi Chen<sup>b</sup>, Chien-Chung Chen<sup>c</sup>

<sup>a</sup> Department of Materials Science and Engineering,  
National Chiao Tung University, 1001 Ta Hsueh Road, Hsinchu, Taiwan 300, ROC

<sup>b</sup> Department of Materials Science and Engineering,  
Minghsin University of Science and Technology, Hsinfong, Hsinchu, 304 Taiwan, ROC

<sup>c</sup> Industrial Technology Research Institute, Hsin Chu, 310, Taiwan, ROC

<sup>d</sup> Department of Materials Science and Engineering, MingDao University, ChangHua 52345, Taiwan, ROC

Available online 14 July 2007

## Abstract

For many years, acid treatment processes have been used to modify substances for their applications on energy storage devices, such as electrochemical capacitors, fuel cells, etc. It is obvious that the increase of surface area and functional groups has beneficial influence on the amount of reactant adsorption. However, the quantitative limitation of active site has been poorly discussed until today. In this experiment, nitric acid (2 M and 14 M) was introduced at 90 °C over different periods of time to oxidate the well-aligned multi-wall carbon nanotubes (MWNTs), which were synthesized directly using carbon cloth (CC) as the substance. Quinoidal functional groups on active CNTs, such as -COOH and -OH, were found to be the result of chemical reaction. Pt catalyst, which was extracted from  $\text{H}_2\text{PtCl}_6 \cdot 6\text{H}_2\text{O}$ , was deposited onto the carbon nanotubes using electroless plating in chloroplatinic acid solution. The extent of Pt adsorption was measured and was substantially larger than the as-prepared CNTs. It was found that the state of quantitative limitation existed in both 2 M and 14 M systems. A model was also developed to illustrate the limitation in the active site due to the chemical oxidation.

© 2007 Elsevier B.V. All rights reserved.

**Keywords:** Modify; Functional group; Adsorption; Nanotube; Limitation

## 1. Introduction

Since carbon nanotubes were first discovered by Iijima [1], it has attracted much attention owing to its novel properties [2–4]. Carbon nanotubes (CNTs) are known to possess exceptional mechanical, electrical and thermal properties, because of their high strength, low density, and high electrical and thermal conductivity [5]. There are numerous potential applications for CNTs, such as flat panel display [6], sensors [7], nanoscale devices [8], vehicles for hydrogen storages [9] and electrochemical energy-storage devices [10]. Especially regarding its application on energy-storage devices, it has drawn much attention to the change in the surface characteristics. It is a common practice to convert the surface bonding into some kinds of functional groups using chemical treatment with

$\text{H}_2\text{SO}_{4(l)}$ ,  $\text{HNO}_{3(l)}$ ,  $\text{KOH}_{(l)}$ , etc. [11–13]. Recently, electrochemical process demonstrated that the functional groups are beneficial towards the uniform separation of deposition [14] and the extent of ion-adsorption [15]. Unfortunately, up to now, the limitation of active site related to chemical oxidation has not been discussed quantitatively.

At the moment, we are aiming at directly fabricating carbon nanotubes onto carbon cloth as the electrodes, and quantitatively illustrate the limitation of chemically oxidized multi-wall carbon nanotubes in the active site, which is related to the adsorption of ions to charge. Physical characteristics of the electrodes will be measured and demonstrated.

## 2. Experimental

Detailed description of the synthesis of multi-wall carbon nanotubes (MWNTs) by microwave plasma-enhanced chemical vapor deposition system (MPECVD), without substrate bias, was reported previously [16]. In this work, carbon cloth (CC,

\* Corresponding author. Tel.: +886 3 5712121x55346; fax: +886 3 5724727.  
E-mail address: [volleyhung@yahoo.com.tw](mailto:volleyhung@yahoo.com.tw) (T.-C. Hung).

typically 2 cm × 2 cm in size) was used as a substrate on account of the flexibility and stability on higher operating voltage. In order to synthesize carbon nanotubes onto CC successfully, we firstly coated Fe as the catalyst on CC by magnetic sputtering. Then the synthesis of carbon nanotubes was processed. For the growth, a mixture of hydrogen and methane, with the gas flow of 90 sccm and 30 sccm respectively, was introduced into the chamber at the pressure of 10 Torr and then it was operated at 300 W. For electrochemically oxidized carbon nanotubes, MWNTs electrode was treated with 2 M and 14 M HNO<sub>3</sub> at 90 °C for different periods of time (0–48 h). Then it was flushed with deionized water repeatedly and purged with N<sub>2</sub> for 10 min.

For the deposition of Pt, the prepared electrodes were immersed in a mixture, which comprise H<sub>2</sub>PtCl<sub>6</sub> · 6H<sub>2</sub>O, PVP-4000 and ethylene glycol, diluted with acetone. PVP is a protection substituted to limit the particle growth spacing. H<sub>2</sub>PtCl<sub>6</sub> · 6H<sub>2</sub>O was used as the precursor of Pt deposition. It was operated at 160 °C for 3 h, followed by filtration with acetone and sintered at 250 °C for 1 h. Measurements were carried out as follows.

The microstructure was respectively observed by means of the JEOL JSM 6500 and JEOL JEM 4000. XPS (ESCA PHI 1600 using an Mg K $\alpha$  X-ray source) and EDX (JEOL

JSM6500F) measurements were carried out for the identification of Pt particles. The functional groups on the surface of oxidized MWNTs can be determined by FTIR on PROTEGE 460 series.

### 3. Results and discussion

Fig. 1(a) shows SEM image of the as-prepared MWNTs fabricated densely onto the carbon cloth. It is well-aligned; having a length and diameter of approximately 20  $\mu$ m and 20 nm, respectively. The TEM image shows hollow structure with amorphous carbon outer surface (outside) and crystalline layers in the inner surface, as can be seen in Fig. 1(c).

Unfortunately, even though the surface area of CNTs is high, it still cannot be completely utilized by physical deposition since this method usually makes the deposition uneven and concentrated on just a part of the surface. On the contrary, the deposition could become uniform by means of the chemical polyol procedure due to the good fluidity and contact with overall area. However, the hydrogen dangling bond on the top surface of the raw MWNTs makes them relatively inert and also makes the agglomeration of particles large in size. In practice, it is important to improve the adhesion efficiency, to make them

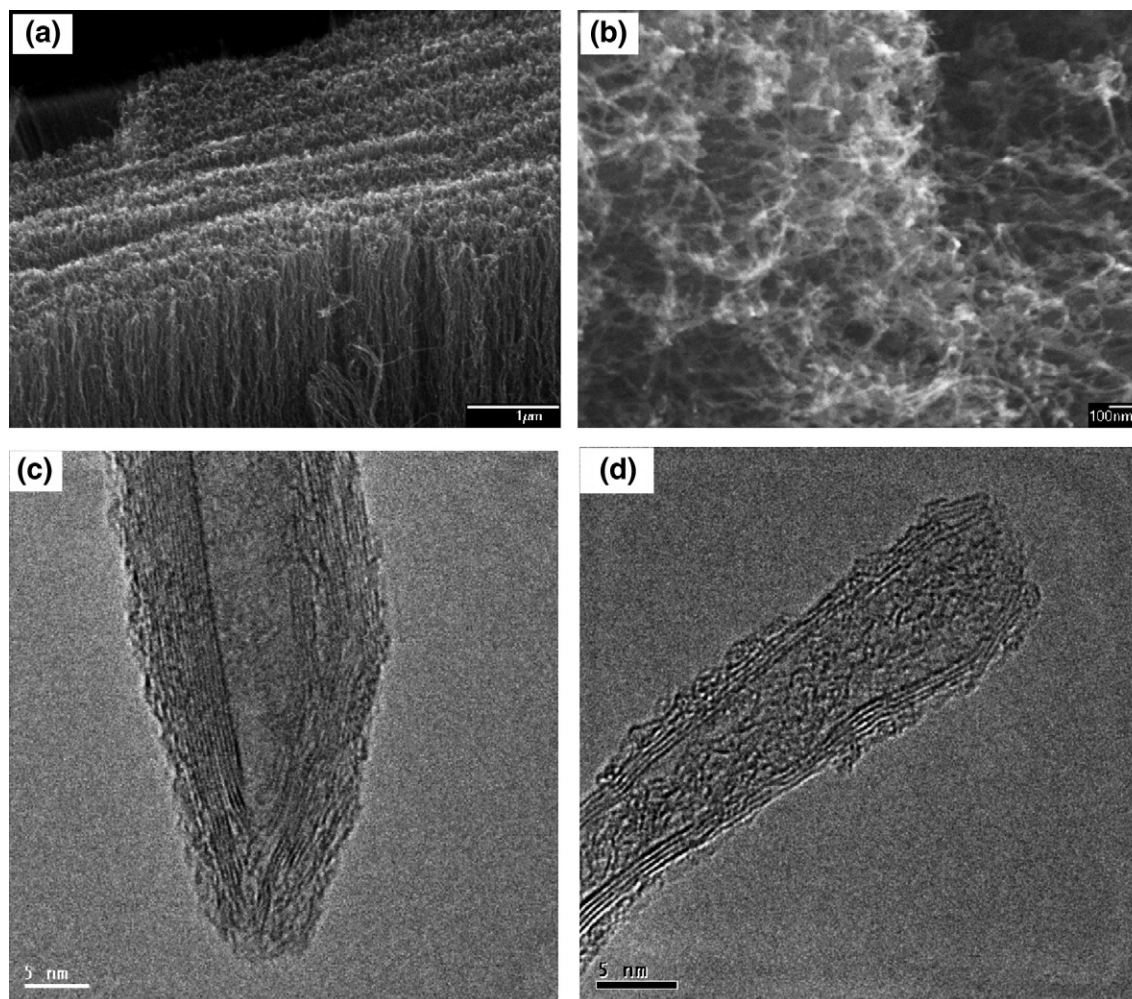


Fig. 1. Typical SEM and TEM images of the MWNTs, synthesized by MPECVD, showed (a, c) before and (b, d) after the chemical oxidation (HNO<sub>3</sub>, 14 M).

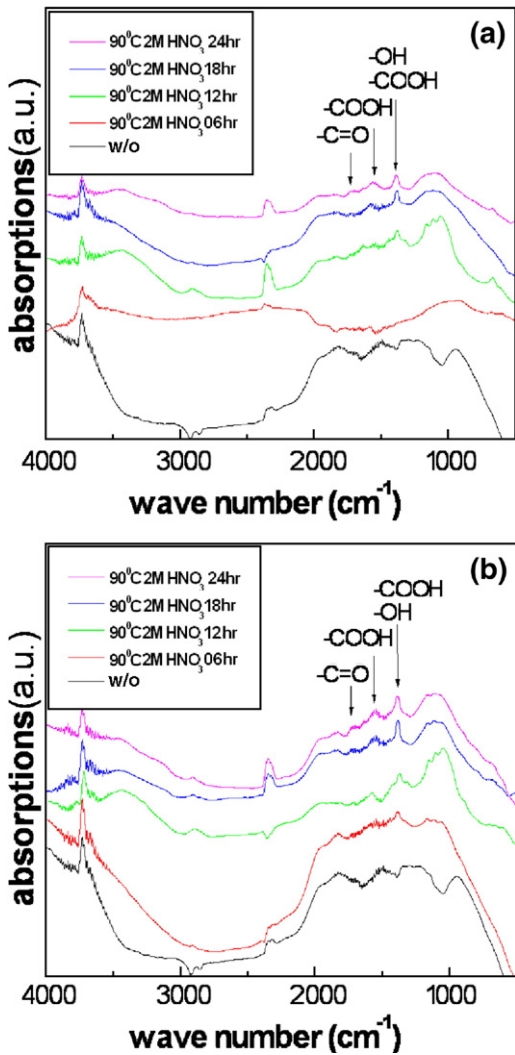


Fig. 2. Infrared spectra of the electrodes treated in various periods of time (0 h–24 h) by (a) 2 M and (b) 14 M  $\text{HNO}_3$ .

uniform and small in size through the surface chemical modification with  $\text{HNO}_3$  solution. As shown in Figs. 1(b) and (d), after the modification with  $\text{HNO}_3$  solution, MWNTs

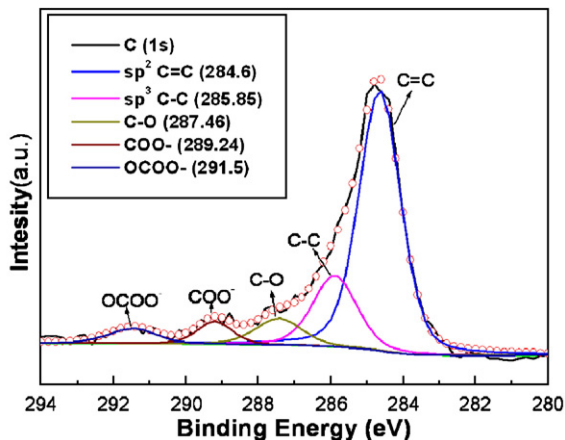
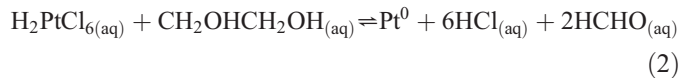


Fig. 3. C 1s spectrum of the  $\text{HNO}_3$ -MWNTs oxidized chemically at 90 °C for 6 h (14 M).

electrode became higher in porosity and severely damaged by the residue of amorphous carbon [17]; and hence the opening at the end of the MWNTs electrode seen here. Such an observation is useful in illustrating the existence of functional groups and larger available surface area [17].

The surface features can be demonstrated by FTIR (Fig. 2) and XPS (Fig. 3). As shown in Fig. 2, a broad intensive band is assigned to the tertiary (-OH) or the carboxylic acids (-COOH) at  $1375\text{ cm}^{-1}$  and to the carboxylic acids (-COOH) at  $1574\text{ cm}^{-1}$  [18]. The carboxyl groups can also be detected by XPS shown in Fig. 3. The C 1s spectrum is composed of C=C ( $\sim 284.6\text{ eV}$ ), C-C ( $\sim 285.85\text{ eV}$ ), CO ( $287.46\text{ eV}$ ), COO- ( $289.24\text{ eV}$ ) and OCOO- ( $\sim 291.5\text{ eV}$ ) functional groups [19]. The observed shift following the chemical treatment is about 1 eV. Thus, the results mentioned above revealed that MWNTs merely form tertiary alcohol (-OH) and the carboxylic acids (-COOH) by  $\text{HNO}_3$  treatment at 90 °C.

The procedure of PVP-protected Pt nanoparticles synthesized in ethylene glycol was presented so that the  $\text{H}_2\text{PtCl}_6$  can be completely reduced at the temperature of 160 °C, explained by Eqs. (1) and (2).



The  $\text{Pt}^{4+}$  ions are reduced to  $\text{Pt}^0$  atoms [20] and it can be identified by the strong  $\text{Pt}_{4f}$  peak, in Fig. 4, obtained from the XPS measurement. After that, the average particle size could be calculated from XRD measurement using the following equation:

$$L = (K\lambda_{K\alpha 1}) / (B_{2\theta} \cos\theta_B)$$

where  $L$  is the average particle size,  $K$  is a constant,  $\lambda_{K\alpha 1}$  being the X-ray wavelength ( $1.54056\text{ \AA}$  for Cu  $K_{\alpha 1}$  radiation),  $B_{2\theta}$  is the peak broadening and  $\theta_B$  is the angle

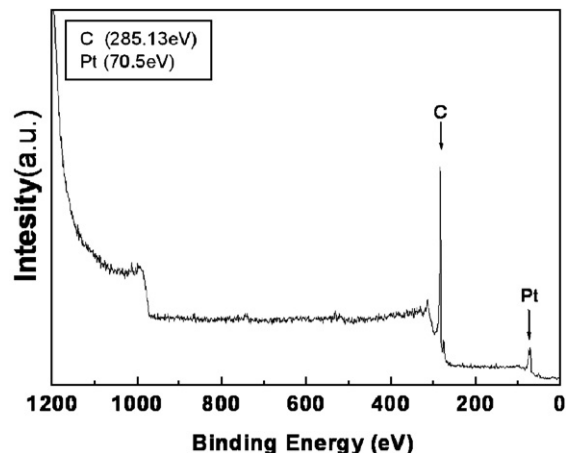


Fig. 4. XPS survey spectrum of the  $\text{HNO}_3$ -MWNTs after the Pt agglomerate.

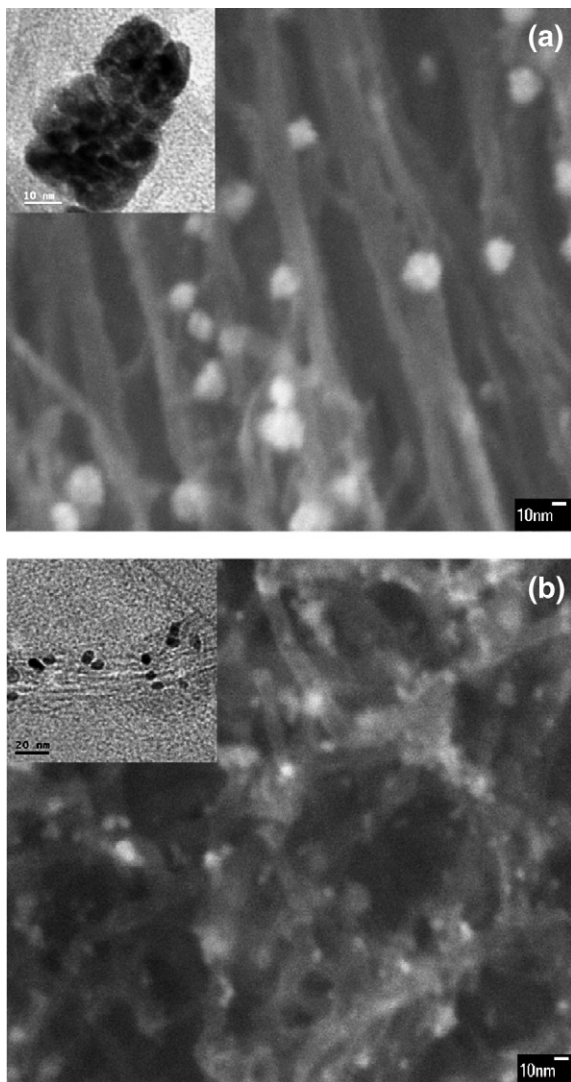


Fig. 5. Typical SEM images; (a) Pt nanoparticles on raw-MWNTs are agglomerated to be a larger nanoparticle and (b) Pt nanoparticles disperse uniformly on  $\text{HNO}_3$ -MWNTs.

corresponding to the peak maximum. Therefore, the average nanoparticle sizes on raw-MWNTs and  $\text{HNO}_3$ -MWNTs are 5.3 nm and 6.7 nm, respectively. However, Fig. 5(a) shows the Pt nanoparticles agglomeration being larger in size on the surface of raw-MWNTs than that which is on the  $\text{HNO}_3$ -MWNTs shown in Fig. 5(b). The Pt nanoparticles could arise uniformly on the integrated MWNTs electrode; furthermore, the particle size corresponding to the  $\text{HNO}_3$ -MWNTs is in a smaller distribution. On top of that, the size of Pt nanoparticle on the  $\text{HNO}_3$ -MWNTs has no distinct difference with regard to the increase of Pt wt.%. It is suggested that these findings arise as a result of the exclusion of adjacent functional groups with the negative charge. In my opinion, the result, especially substantial and uniform deposition, has a beneficial influence on the application of energy-storage devices, such as the direct methanol fuel cell (DMFC).

Fig. 6 directly shows the evidence that the quantity of Pt, loaded on MWNTs with reference to carbon, can be estimated

to be 14.37/16.72/24.38/28.21/26.99 wt.% and 5.38/26.52/27.94/25.79/25.95 wt.%, in regard to the chemical modification of 2 M and 14 M  $\text{HNO}_3$  respectively, within the particular periods of oxidation. The trend observed is that the quantity of Pt increases up to a certain point in time, then there is no distinct deviation afterwards. It reveals that relatively large quantity of Pt could be obtained after 12 h and 6 h using 2 M  $\text{HNO}_3$ -MWNTs and 14 M  $\text{HNO}_3$ -MWNTs respectively, as shown in Figs. 6(a) and (b). They also showed the results of Pt active surface area of these two electrodes. Due to the influence of the exclusion of functional groups mentioned above, the active surface area would be significantly different following the  $\text{HNO}_3$  treatment. This confirms that the treatment can be adopted to express the quantitative limitation of active site more effectively. We suppose that other usages of chemical oxidization, such as the microwave digestion system [21], also exhibit the same result. It is noticeable that the accurate quantity of Pt is difficult to be measured.

A hypothetical model is developed in Fig. 7 to illustrate the process and result of the quantitative limitation. The fresh functional groups would reform on the new sites in the inner layer of  $\text{HNO}_3$ -MWNTs even though functional groups on the outer layer surface are removed as time passes by, with the consumption of the outer layer which is comprised of

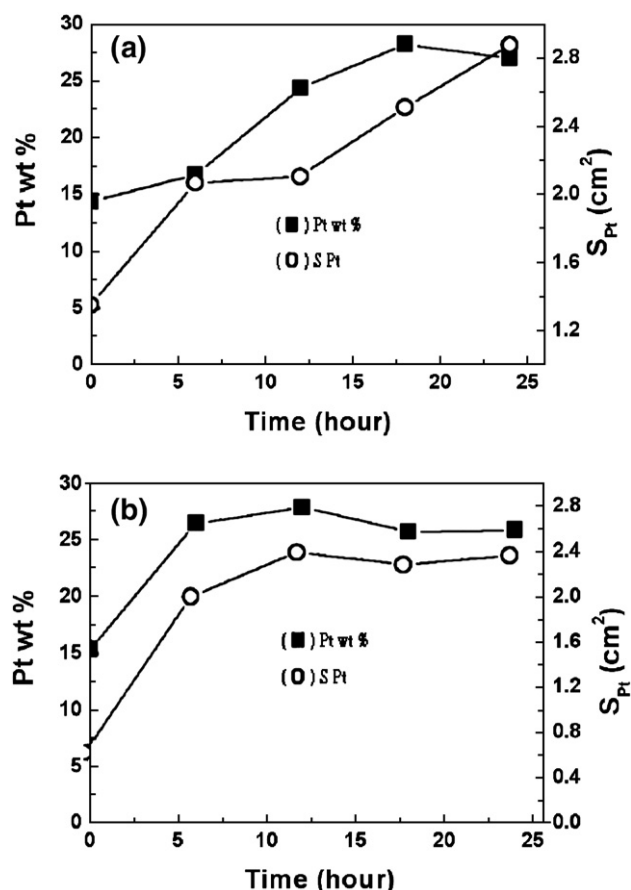


Fig. 6. Period of chemical oxidation (0 h–24 h) to active surface area and to Pt wt.%, which is measured by EDX-mapping; (a) 2 M, (b) 14 M.

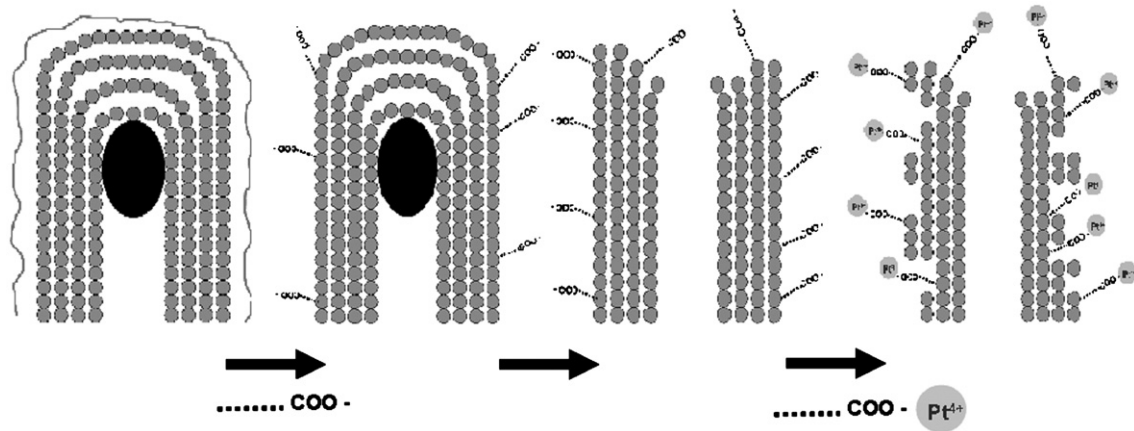


Fig. 7. The diagram of hypothetical model for the quantitative limitation of active site.

amorphous and crystalline carbon. Therefore, the total number of functional groups is kept stable during the space of time.

#### 4. Conclusion

In conclusion, in this study, the supporting of well-aligned MWNTs for Pt has advantages of including more anchoring sites and lots of functional groups by using the electrochemical oxidization to attract ions from the caps, sidewalls and particularly the inner parts of MWNTs. The length and diameter of the aligned MWNTs are approximately 20  $\mu\text{m}$  and 20 nm, respectively. After the modification with higher concentration of  $\text{HNO}_3$  at 90  $^\circ\text{C}$ , the integrated MWNTs electrode becomes higher in porosity due to the action of the residues of amorphous carbon, which is shown on the end opening. The results of the FTIR and XPS analysis reveal that the surface of MWNTs behaves in such a way which indicates the existence of tertiary alcohol ( $-\text{OH}$ ) and the carboxylic acids ( $-\text{COOH}$ ). Therefore, these functional groups contribute to the accumulation of smaller and more uniform Pt nanoparticles on the activated MWNTs. A relatively large quantity of Pt, both with 2 M  $\text{HNO}_3$ -MWNTs and 14 M  $\text{HNO}_3$ -MWNTs, could be obtained after a period of time of about 12 h and 6 h, respectively. Furthermore, the stable quantity of Pt related to the active site increases and a model is developed to illustrate the quantitative limitation caused by the typical chemical oxidization. The approach outlined in this study should be replicated in other manufacturing processes and be put to significant applications.

#### References

- [1] S. Iijima, Nature 354 (1991) 56.
- [2] T.M. Whitney, J.S. Jiang, P.C. Searson, C.L. Chien, Science 261 (1993) 1316.
- [3] M.M.J. Treacy, T.W. Ebbenson, J.M. Gibson, Nature 381 (1996) 678.
- [4] P. Delaney, H.J. Choi, J. Ihm, S.G. Louie, M.L. Cohen, Nature 391 (1998) 466.
- [5] T.W. Ebbesen, Carbon Nanotubes: Preparation and Properties, CRC Press, Boca, Raton, FL, 1997.
- [6] W.B. Choi, Y.W. Jin, H.Y. Kim, S.J. Lee, M.J. Yun, J.H. Kang, Y.S. Choi, N.S. Park, N.S. Lee, J.M. Kim, Appl. Phys. Lett. 78 (2001) 1547.
- [7] J. Kong, N.R. Franklin, C. Zhou, M.G. Chapline, S. Peng, K. Cho, H. Dai, Science 287 (2000) 622.
- [8] P.G. Collins, A. Zettl, H. Bando, A. Thess, R.E. Smalley, Science 278 (1997) 100.
- [9] C. Liu, Y.Y. Fan, M. Liu, H.T. Cong, H.M. Cheng, M.S. Dresselhaus, Science 286 (1999) 1127.
- [10] A.G. Pandolfo, A.F. Hollenkamp, J. Power Sources 157 (2006) 11.
- [11] K. Jurewicz, K. Babel, A.Z'io' 1 kowski, H. Wachowska, Electrochim. Acta 48 (2003) 1491.
- [12] K. Babel, K. Jurewicz, J. Phys. Chem. Solids 65 (2004) 275.
- [13] K. Kierzek, E. Frackowiak, G. Lota, G. Gryglewicz, J. Machnikowski, Electrochim. Acta 49 (2004) 1169.
- [14] N.M. Rodriguez, M.S. Kim, R. Terry, K. Baker, J. Phys. Chem. 98 (1994) 13108.
- [15] Y.C. Liu, X.P. Qiu, Y.Q. Huang, W.T. Zhu, J. Power Sources 111 (2002) 160.
- [16] C.F. Chen, C.L. Lin, C.M. Wang, Thin Solid Films 444 (2003) 64.
- [17] J.S. Ye, X. Liu, H.F. Cui, W.D. Zhang, F.S. Sheu, T.M. Lim, Electrochem. Commun. 7 (2005) 249.
- [18] K.C. Park, T. Hayashi, H. Tomiyasu, M. Enbo, M.S. Dresselhaus, J. Mater. Chem. 15 (2005) 407.
- [19] T.I.T. Okpalugo, P. Papakonstantinou, H. Murphy, J. McLaughlin, N.M.D. Brown, T. McNally, Fuller. Nanotub. and Carbon Nanostructures 13 (2005) 477.
- [20] T. Teranishi, M. Hosoe, T. Tanaka, M. Miyake, J. Phys. Chem., B 103 (1999) 3818.
- [21] C.M. Chen, M. Chen, F.C. Leu, S.Y. Hsu, S.C. Wang, S.C. Shi, C.F. Chen, Diamond and Related Materials 13 (2004) 1182.